2920 *Chem. Mater.* **2009,** *21,* 2920–2929
DOI:10.1021/cm900641s

CHEMISTRY OF MATERIALS
Article

Design of Highly Dense Boron Nitride by the Combination of Spray-Pyrolysis of Borazine and Additive-Free Sintering of Derived Ultrafine Powders

Vincent Salles,[†] Samuel Bernard,*[,†]
Junping Li,[†] Arnaud Brioude,[†] Sirine Chehaidi,[‡] Sylvie Foucaud,[‡] and Philippe Miele[†]

[†]*Laboratoire des Multimateriaux et Interfaces (UMR CNRS 5615), Université Lyon 1, Université de Lyon, 43 bd du 11 Novembre 1918, 69622 Villeurbanne Cedex, France, and* [‡]*SPCTS (UMR CNRS 6638), Faculté des Sciences et Techniques, 123 Avenue Albert Thomas, 87060 Limoges, France*

Received March 6, 2009. Revised Manuscript Received April 20, 2009

Ultrafine boron nitride ($B_{1.0}N_{0.9}$) powders have been prepared by the spray-pyrolysis of borazine and then used to explore their potentialities to form three-dimensional boron nitride ($B_{1.0}N_{\sim 1.0}$) by additive-free conventional sintering. Complete characterization of the $B_{1.0}N_{0.9}$ powders by SEM, HRTEM, X-ray diffraction (XRD), infrared spectroscopy (FTIR), and Raman demonstrated that samples form elementary blocks containing slightly agglomerated nanocrystalline particles with sizes ranging from 55 to 120 nm. On the basis of the BET specific surface area (SSA; 34.6 ± 0.7 $m^2\ g^{-1}$) and the helium density of powders (d = 1.95 ± 0.02 g cm^{-3}), an average particle size (APS) of 89 nm has been calculated. Ultrafine $B_{1.0}N_{0.9}$ powders were successfully used to design microstructured disk-shaped boron nitride materials with a very high relative density (96.3%), a homogeneous microstructure, and an average hardness throughout the cross-section of 8 HV (78 MPa) at a temperature (1840 °C) lower than those currently applied to sinter boron nitride with sintering additives. Sintering resulted in the orderly arrangement of the boron nitride platelets parallel to the pressing direction.

Introduction

Boron nitride is a synthetic binary compound discovered in the early 19th century which proposes similarities in its crystal structure with carbon.[1] In the same way that carbon exists as graphite and diamond, boron nitride can be synthesized in a layered (hexagonal; *h*-BN) or a tetrahedrally (cubic; *c*-BN) structure. The former, in which the in-plane atoms are bonded through localized sp^2 hybridization while the out-of-plane layers are bonded by delocalized weak π orbital, displays interesting properties for many technical applications. The layered lattice structure of *h*-BN provides good lubricating properties; it is stable at high temperature (at least 2000 °C) in a nitrogen atmosphere, is not wetted by most molten metals, glasses, and salts, and hence has a high resistance to chemical attack; and it displays high dielectric breakdown strength, high volume resistivity, and good resistance to oxidation. Therefore, it is usually prepared as hot (isostatic) pressed shaped parts to be used as thermocouple protection sheaths, crucibles, and linings for reaction vessels.[2]

The preparation of dense bulk boron nitride is conventionally achieved by nitridation of boric oxide followed by sintering at elevated temperatures.[3] Beside the fact that the use of boric oxide as a precursor inherently induces the presence of boron oxynitride phases BN_xO_y in the derived BN material,[4] a first disadvantage of the sintering process of boron nitride lies in the use of sintering additives which remain as a second phase in the resulting materials. The second disadvantage is the limitation to design the material structure at nanoscale using this conventional solid-state route. These drawbacks negatively influence the properties of the sintered material and therefore encourage research groups to seek alternative strategies which supply pure, highly dense, and even nanostructured bulk materials.

It is now clearly established that enhanced physical and chemical properties as well as unusual properties can be generated when the composition of the desired material is controlled and fixed at atomic scale in the

*To whom correspondence should be addressed. E-mail: samuel.bernard@univ-lyon1.fr. Tel: +33 472 433 612. Fax: +33 472 440 618.

(1) Bolmain, W. H. *J. Prakt. Chem.* **1842**, *27*, 422–430.
(2) Paine, R. T.; Narula, C. K. *Chem. Rev.* **1990**, *90*, 73–91.
(3) (a) Mandorf, V., Jr.; Montgomery, L. C. U.S. Patent 3,734,997, May 22, **1973**. (b) Hubacek, M.; Ueki, M.; Sato, T. *J. Am. Ceram. Soc.* **1996**, *79*, 283–285. (c) Hubacek, M.; Ueki, M. *J. Am. Ceram. Soc.* **1999**, *82*, 156–160. (d) Jacobson, N.; Farmer, S.; Moore, A.; Sayir, H. *J. Am. Ceram. Soc.* **1999**, *82*, 393–398.
(4) Economy, J.; Anderson, R. V.; Matkovich, V. I. *Appl. Polym. Symp.* **1969**, 377–386.

Published on Web 06/12/2009

starting precursor and the dimensions of at least one of the constituents of the desired material are reduced to the nanometric scale.[5,6] These two requirements taken together provide great interests to prepare nanocomposites by combining two phases (one being at nanometer scale) with distinct attributes[7] or macroscopic sintered materials in the desired composition.[8] In particular, one of the present challenges in material science to fabricate large-scale nanostructured components is focused on the use of powders with particle sizes reduced to the nanometric scale to be sintered, while maintening the structure at a nanometric scale throughout consolidation.

The synthesis of *h*-BN powders with small sizes has already been reported using various methods. The preparation of BN powders was first reported in 1990.[9] In this patent, authors prepared powders with small sizes (< 1 μm) through low-temperature chemical vapor deposition using boron trichloride (BCl_3) and ammonia (NH_3). However, as-prepared powders with helium density in the range 1.6−1.9 g cm^{-3} contained impurities such as oxygen and carbon which are known to alter the properties of the material. Using the same precursors, powders with small sizes and high BET specific surface area (from 185 to 234 m^2 g^{-1}) were synthesized by heating the precursors through a high powered continuous wave CO_2 laser.[10] Nanometric boron nitride powders have been deposited on specific substrates by PECVD from a borane−ammonia mixture, but the material contained a large quantity of hydrogen.[11] These processes are usually very complex and require heavy equipment which drastically increase the cost of the resulting materials. Intensive efforts have been made by Paine et al.[12] These authors used an aerosol assisted vapor synthesis from liquid ammonia solutions of poly(borazinylamine), from boric acid as well as from organoborate precursors. For all the employed precursors, the BN powders, which were mesoporous in some cases,[12e] exhibited spherical morphologies, final sizes of ~1 μm, and relatively low oxygen and carbon contents, but a postpyrolysis annealing was required to reach these reduced proportions of oxygen and carbon. Following a similar strategy, Bando et al. prepared submicrometer spherical BN particles with diameters ranging from 50 to 400 nm by using a two-step synthetic process from solution of trimethoxyborane (or trimethyl borate).[13a] No traces of carbon and oxygen have been detected by EELS as mentioned in ref 13a. However, in a more recent article,[13b] Tang et al. admitted that they could not obtain oxygen-free BN particles by the CVD process from trimethoxyborane with ammonia followed by a second-stage ammonia annealing, even at 1400 °C. Oxygen-free BN particles could be generated using argon instead of ammonia during the second stage of the process.[13b] Another article reported the preparation of boron nitride particles through a two-step process. Shi et al. synthesized hexagonal boron nitride particles in the diameter range 0.5−1.5 μm by spray-drying a mixture of HBO_3 and $Na_2B_4O_7$ at 250 °C which was subsequently mixed with $(NH_2)_2CO$ to be heated in air at 900 °C. As-made particles were nitrided at different temperatures from 1200 to 1500 °C.[14] More recently, Sneddon et al. synthesized freestanding pure boron nitride particles (~8−10 μm in diameter) with micro- and nanoscale features using frustules of diatoms as microscale nanostructured templates and soluble polyborazylene as starting precursor.[15a]

A reliable single-step powder synthesis process leading to the synthesis of highly pure ultrafine powders (~100 nm) from a single-source precursor is not available today. Furthermore, no attempts have been made on the sintering of the powders which are described in the previously quoted articles. Within this context, we propose a two-stage methodology which uses in a first stage a spray-pyrolysis (SP) process for the synthesis of ultrafine boron nitride powders and in a second stage a conventional sintering process of the latter for consolidation of the three-dimensional boron nitride material. The first part of the present paper reports a single-step access to ultrafine BN powders by combining a liquid oxygen-free precursor synthesis with a SP process. The oxygen-free precursor approach is the only solution to produce high

(5) (a) Riedel, R.; Mera, G.; Hauser, R.; Klonczynski, A. *J. Ceram. Soc. Jpn.* **2006**, *114*, 425–444. (b) Duperrier, S.; Gervais, C.; Bernard, S.; Cornu, D.; Babonneau, F.; Balan, C.; Miele, P. *Macromolecules* **2007**, *40*, 1018–1027. (c) Bernard, S.; Fiaty, K.; Cornu, D.; Miele, P.; Laurent, P. *J. Phys. Chem. B* **2006**, *110*, 9048–9060.
(6) (a) Jiang, L.; Gao, L. *J. Mater. Chem.* **2005**, *15*, 260–266. (b) Yang, W.; Araki, H.; Tang, C.; Thaveethavorn, S.; Kohyama, A.; Suzuki, H.; Noda, T. *Adv. Mater.* **2005**, *17*, 1519–1523. (c) Salles, V.; Foucaud, S.; Laborde, E.; Champion, E.; Goursat, P. *J. Eur. Ceram. Soc.* **2007**, *27*, 357–366. (d) Salles, V.; Foucaud, S.; Goursat, P.; Champion, E. *J. Eur. Ceram. Soc.* **2008**, *28*, 1259–1266.
(7) (a) Li, Y.; Fernandez-Recio, L.; Gerstel, P.; Srot, V.; Van Aken, P. A.; Kaiser, G.; Burghard, M.; Bill, J. *Chem. Mater.* **2008**, *20*, 5593–5599. (b) Cai, Y.; Shah, S. R.; Zimmermann, A.; Weinmann, M.; Raj, R.; Aldinger, F. *Phys. Status Solidi* **2002**, *193*, R13–R15. (c) Kokott, S.; Heymann, L.; Motz, G. *J. Eur. Ceram. Soc.* **2008**, *28*, 1015–1021.
(8) (a) Ishihara, S.; Gu, H.; Bill, J.; Aldinger, F.; Wakai, F. *J. Am. Ceram. Soc.* **2002**, *85*, 1706–1712. (b) Hungria, T.; Alguero, M.; Hungria, A. B.; Castro, A. *Chem. Mater.* **2005**, *17*, 6205–6212. (c) Leconte, Y.; Maskrot, H.; Herlin-Boime, N.; Porterat, D.; Reynaud, C.; Gierlotka, S.; Swiderska-Sroda, A; Vicens, J. *J. Phys. Chem. B* **2006**, *110*, 158–163. (d) Zhang, L.; Elwazri, A. M.; Zimmerly, T.; Brochu, M. *Mater. Sci. Eng.* **2008**, *A487*, 219–227. (e) Buscaglia, M. T.; Viviani, M.; Zhao, Z.; Buscaglia, V.; Nanni, P. *Chem. Mater.* **2006**, *18*, 4002–4010. (f) Hungria, T.; Alguer, M.; Castro, A. *Chem. Mater.* **2006**, *18*, 5270–5376.
(9) Iltis, A.; Maguier, C. Eur. Patent 396,448, July 11, **1990**.
(10) Baraton, M. I.; Boulanger, L.; Cauchetier, M.; Lorenzelli, V.; Luce, M.; Merle, P.; Quintard, P.; Zhou, Y. H. *J. Eur. Ceram. Soc.* **1994**, *13*, 371–378.
(11) Costa, J.; Sardin, G.; Campmany, J.; Bertran, E. *Vacuum* **1994**, *45*, 1115–1117.
(12) (a) Lindquist, D. A.; Kodas, T. T.; Smith, D. M.; Xiu, X.; Hietala, S. L.; Paine, R. T. *J. Am. Ceram. Soc.* **1991**, *74*, 3126–3128. (b) Pruss, E. A.; Wood, G. L.; Kroenke, W. J.; Paine, R. T. *Chem. Mater.* **2000**, *12*, 19–21. (c) Wood, G. L.; Janik, J. F.; Visi, M. Z.; Schubert, D. M.; Paine, R. T. *Chem. Mater.* **2005**, *17*, 1855–1859. (d) Wood, G. L.; Janik, J. F.; Pruss, E. A.; Dreissig, D.; Kroenke, W. J.; Habereder, T.; Nöth, H.; Paine, R. T. *Chem. Mater.* **2006**, *18*, 1434–1442. (e) Wood, G. L.; Paine, R. T. *Chem. Mater.* **2006**, *18*, 4716–4718.
(13) (a) Tang, C.; Bando, Y.; Golberg, D. *Chem. Commun.* **2002**, 2826–2827. (b) Tang, C.; Bando, Y.; Huang, Y.; Zhi, C.; Golberg, D. *Adv. Funct. Mater.* **2008**, *18*, 3653–3661.
(14) Shi, X.; Wang, S.; Yang, H.; Duan, X.; Dong, X. *J. Solid State Chem.* **2008**, *181*, 2274–2278.

purity and chemically homogeneous nanostructured boron nitride,[16−21] while SP, known to be a cost-effective powerful technique, offers a tremendous versatility in terms of compositions, morphologies, and sizes.[22] Borazine was selected as a single-source molecular precursor. It is currently used as a molecular precursor to prepare inorganic polymers, polyborazylene or analogues, then shaped-boron nitride materials including micropowders, fibers, and nanotubes/wires.[15−17] Furthermore, it represents a suitable liquid candidate with an adequate vapor pressure to be used in CVD-based processes and produce nanomeshs and nanotubes.[18−21] In a second part of this paper, we demonstrate that borazine-derived $B_{1.0}N_{0.9}$ powders are appropriate candidates for consolidation of microstructured boron nitride materials with the desired purity ($B_{1.0}N_{\sim 1.0}$) and a very high density through an additive-free sintering process.

Experimental Section

Materials. The synthesis of borazine was carried out in an argon atmosphere, using argon/vacuum lines, and Schlenk-type flasks. Argon (>99.995%) was purified by passing through successive columns of phosphorus pentoxide, siccapent, and BTS catalysts. Schlenks were dried at 120 °C overnight before pumping under vacuum and filling them with argon for the synthesis. Sodium borohydride ($NaBH_4$, ≥98.5%, powder from Sigma-Aldrich), ammonium sulfate ($(NH_4)_2SO_4$, ≥99.0% from Sigma-Aldrich), and tetraethylene glycol dimethyl ether ($CH_3O(CH_2CH_2O)_4CH_3$, 99.0% from Sigma-Aldrich) were used as-received. It should be mentioned that ammonium sulfate was dried at 120 °C inside an oven for three days and then put under vacuum during cooling for 1 h. Manipulation of the chemical products was made inside an argon-filled glovebox (Jacomex BS521; Dagneux, France) dried with phosphorus pentoxide.

Borazine Synthesis. The operating procedure, adapted from the literature,[23] was previously reported in our paper.[16] IR (CsI windows/cm^{-1}): ν(N−H) = 3451 m; ν(B−H) = 2509 m; ν(B−N) = 1454 s; δ(B−N−B) = 897 m. ^{1}H NMR (300 MHz/$CDCl_3$/ppm): δ = 3.30−5.35 (quadruplet, 3H, B*H*), 5.35−6.05 (triplet, 3H, N*H*). ^{11}B NMR (96.29 MHz/C_6D_6/ppm): δ = 30.1 (br).

Ultrafine Powder Preparation. The SP process has been described in detail in our previously published papers.[6c,6d] The experimental setup (Figure 1) is composed of a nebulized spray generator (RBI, Meylan, France), where the spray is generated by a piezoelectric device (barium titanate). Frequency (800 kHz) and power (100 W) alimentations were adjusted to obtain the aerosol. The aerosol temperature was first held at 15 °C by a regulated water circulation to avoid borazine evaporation and/or condensation.

The piezoelectric device generated an ultrasound beam which was directed to the liquid−gas interface; a fountain formed at the surface followed by the generation of the spray resulting from vibrations at the liquid surface and cavitations at the gas−liquid interface.[24] The borazine was directly introduced in the aerosol generating chamber under nitrogen, then aerosolized and carried to the pyrolysis furnace with a 0.5 mL min^{-1} nitrogen flow rate. The thermal decomposition of borazine was performed in a hot alumina tube containing an isothermal zone of 0.1 m in length. The fast heating rate implied gaseous species generation leading to powder formation by a chemical vapor condensation route. The particles were finally trapped into two collectors placed before the vacuum pump and containing filter-barriers made of microporous alumina (pore size of 1 μm). Yield was estimated to be 0.22 g min^{-1}. After their synthesis, trapped powders were stored inside an argon-filled glovebox. In a typical experiment, 27 mL (21.9 g) of borazine are used to produce 6.5 g of white color powders. However, the exact yield is difficult to estimate because of the design of the SP system. A non-negligible quantity of powders, deposited in the furnace tube, could not be recovered. Anal. Found (wt %): H, <0.3; B, 44.4; N, 54.7; O, 0.8 [$B_{1.0}N_{0.9}$ by omitting hydrogen and oxygen contents]. Calcd (wt %): B, 43.56; N, 56.44.

Sintering Process. Ultrafine powders were used to process bulk boron nitride. Preparation of samples for sintering was performed inside an argon-filled glovebox. A total of 1.5 g of powders were processed by conventional sintering in nitrogen, at 0.1 T as thin disks of 16 mm diameter into a graphite mold. Papyex foils were placed between BN powders and graphite to avoid carbon contamination of the nanopowders. The disks were then hot pressed under 0.1 T under vacuum up to 600 °C before switchingthe vacuum to nitrogen atmosphere. Above 1100 °C, the temperature was automatically monitored and regulated by an optical pyrometer focused on the surface of the die, and a load of 40 MPa was applied. After a dwelling time of 1 h at 1840 °C, the furnace was allowed to cool down at 8 °C·min^{-1} with a gradual removal of the load (up to RT) to avoid the appearance of cracks in the piece.

Characterization. Bulk compositional evolution of powders was made by the Service Central de Microanalyse de Vernaison (Vernaison, France) for boron, carbon, and hydrogen and in the SPCTS lab (Limoges, France) for nitrogen and oxygen elements. The methods included thermal decomposition of powders under oxygen to measure carbon and hydrogen contents, under inert atmosphere for the measurement of nitrogen and oxygen contents, and by ICP for boron content. In addition, powders were analyzed by energy-dispersive X-ray (EDX). An EDX system EDAX Genesis 4000 coupled with a SEM (Hitachi S800) was used to quantify boron, nitrogen, oxygen, and carbon elements. As-prepared BN powders were characterized and analyzed by a transmission electron

(15) (a) Kusari, U.; Bao, Z.; Cai, Y.; Ahmad, G.; Sandhage, K. H.; Sneddon, L. G. *Chem. Commun*. **2007**, 1177–1179. (b) Fazen, P. J.; Beck, J. S.; Lynch, A. T.; Remsen, E. E.; Sneddon, L. G. *Chem. Mater*. **1990**, *2*, 96–97. (c) Fazen, P. J.; Remsen, E. E.; Caroll, P. J.; Beck, J. S.; Sneddon, L. G. *Chem. Mater*. **1995**, *7*, 1942–1956. (d) Wideman, T.; Sneddon, L. G. *Chem. Mater*. **1996**, *8*, 3–5. (e) Wideman, T.; Remsen, E. E.; Cortez, E.; Chlanda, V. L.; Sneddon, L. G. *Chem. Mater*. **1998**, *10*, 412–421.
(16) Bechelany, M.; Bernard, S.; Brioude, A.; Stadelmann, P.; Charcosset, C.; Fiaty, K.; Cornu, D.; Miele, P. *J. Phys. Chem. C* **2007**, *111*, 13378–13384.
(17) Wang, Y; Shimada, S; Yamamoto, Y; Miyaura, N. *Mater. Res. Bull*. **2008**, *43*, 251–256.
(18) Goriachko, A.; He, Y.; Knapp, M.; Over, H.; Corso, M.; Brugger, T.; Berner, S.; Osterwalder, J.; Greber, T. *Langmuir* **2007**, *23*, 2928–2931.
(19) Corso, M.; Auwärter, W.; Muntwiler, M.; Tamai, A.; Greber, T.; Osterwalder, J. *Science* **2004**, *303*, 217–220.
(20) Lourie, O. R.; Jones, C. R.; Bartlett, B. M.; Gibbons, P. C.; Ruoff, R. S.; Buhro, W. E. *Chem. Mater*. **2000**, *12*, 1808–1810.
(21) Kim, M. J.; Chatterjee, S.; Kim, S. M.; Stach, E. A.; Bradley, M. G.; Pender, M. J.; Sneddon, L. G.; Maruyama, B. *Nano Lett*. **2008**, *8*, 3298–3302.
(22) (a) Kim, M.; Hinklin, T. R.; Laine, R. L. *Chem. Mater*. **2008**, *20*, 5154–5162. (b) Bang, J. H.; Helmich, R. J.; Suslick, K. S. *Adv. Mater*. **2008**, *20*, 2599–2603.
(23) Wideman, T.; Sneddon, L. G. *Inorg. Chem*. **1995**, *34*, 1002–1003.
(24) Langlet, M.; Joubert, J. C. In Chemistry of Advanced Materials − A Chemistry for the 21st Century; Rao, C. N. R., Ed.; IUPAC, Blackwell Scientific: Oxford, U.K., 1993; p 55.

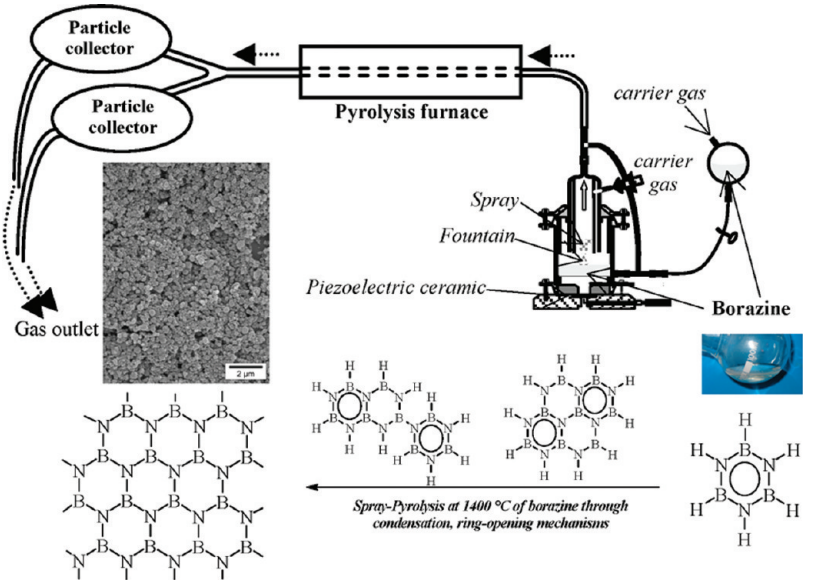

Figure 1. SP setup (SEM micrograph of borazine-derived powders, inset).

microscopy (TEM) with a TOPCON 002B working at 200 kV. Samples were characterized using a Philipps PW 3040/60 X'Pert PRO X-ray diffraction system. Powder samples were prepared by placing ~100 mg on the XRD sample holder (PVC), and the sintered pieces were put down on the XRD sample holder for data collection. Cu Kα (λ = 1.54 Å) radiation with a Ni filter was used with a working voltage and a current of 40 kV and 30 mA, respectively. Scans were continuous from 10 to 90° 2θ for powders and 20−80° 2θ for sintered boron nitride with a time per step of 0.85 s in increments of 0.017° 2θ. Peak positions and relative intensities were characterized by comparison with JCPDS files of the standard material (JCPDS card No. 34−0421). Debye−Scherrer line broadening was used to calculate the average crystallite sizes (ACS) from each XRD pattern. Infrared spectroscopy of powders and derived 3D materials was taken with a Nicolet 380 FT-IR spectrometer coupled with the attenuated total reflectance (ATR) accessory. It should be mentioned that the FTIR spectrum of borazine was recorded from a Nicolet Magna 550 Fourier transform infrared spectrometer by introducing the liquid molecule between two KBr windows. A Renishaw model RM 1000 Raman microscope operating at lambda = 514.5 nm was used for Raman spectroscopy. The specific surface area (SSA) of powders was measured on a Micromeritics-ASAP 2010, BET 8 pts. Samples (450 mg) were degassed at 250 °C for 12 h. Analysis was run at 77 K with N_2. The BET specific surface area was calculated from the nitrogen adsorption data in the relative pressure range from 0.05 to 0.3. The true densities of powders and derived bulk samples were measured by helium pycnometry (Micromeritics AccuPyc 1330) from approximately 100 mg of samples. The SSA and true density of powders were used to calculate the average particle size (APS). The microstructure of sintered boron nitride was characterized on polished surfaces (up to 9 μm silicon carbide) by scanning electron microscopy (SEM) and optical microscopy with Hitachi S800 scanning electron microscopy and Olympus BX60 optical apparatus, respectively. The hardness was measured on the monolith surface with a Vickers indentor (Model ZWICK Materialprüfung 312002/00 instrument). Several measurements were performed using a load of 0.3 kg applied during 15 s.

Results and Discussion

The objectives of the current study are to detail the synthesis and characterization of ultrafine boron nitride powders which have been synthesized through a single step access and then explore their potentialities for sintered boron nitride preparation.

Powder Synthesis. Compared to other techniques which have been used to produce boron nitride powders, the proposed SP route does not require the use of organic solvent and/or ammonia atmosphere during pyrolysis. Furthermore, according to the fact that there is clear phenomenological evidence that the ceramic retains a memory of its molecular origin, we focused on a rational design criterion to our choice of precursors, that is, use of chloride-, oxygen-, and carbon-free inorganic precursors, and we choose borazine. Referring to its chemical formula $H_3B_3N_3H_3$ and structure, borazine represents a single-source molecule with both boron and nitrogen elements in the correct boron-to-nitrogen ratio and symmetry. In addition, it offers the advantage of being fluid with an adequate vapor pressure which can be sprayed to generate ultrafine boron nitride powders in inert atmosphere.

Borazine was prepared and purified similarly to the procedure developed by Wideman and Sneddon.[23] ^{1}H NMR confirmed the purity of the as-synthesized molecule through the appearance of the BH quadruplet between 3.30 and 5.35 ppm and the NH triplet between 5.35 and 6.05 ppm (Supporting Information SI.1). The experimental SP setup consists of an aerosol/generator producing precursor droplets, a tube furnace equipped with an alumina tube, (1400 °C) along with appropriate mass flow controllers that allow for the continuous delivery of the borazine aerosol into the hot-zone through a controlled flow rate of the carrier gas (nitrogen). The experimental setup for SP is shown in Figure 1 (see Experimental Section for details).

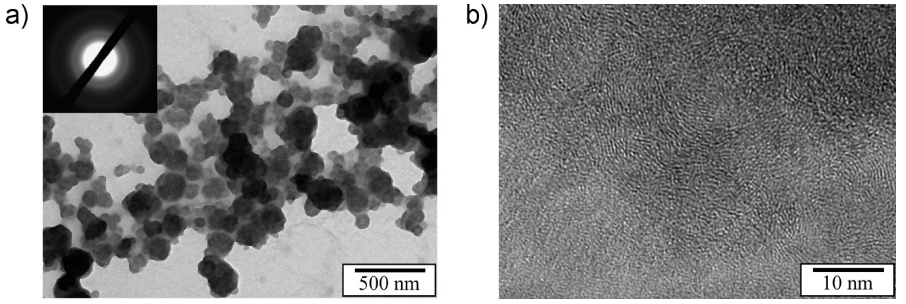

Figure 2. TEM micrographs of as-synthesized ultrafine powders (SAED, inset of part a).

The borazine exhibited an excellent ability to be sprayed and then pyrolyzed at 1400 °C in a nitrogen atmosphere to produce boron nitride powders. Keeping in mind that the borazine is unstable at RT, the temperature of the aerosol generating chamber was maintained at 15 °C during the whole experiment (30 min). As a confirmation of the stability of borazine at 15 °C, FTIR and ^{1}H NMR spectra of the recovered borazine did not change after experiments (Supporting Information SI.1). The chemistry involved during the borazine-to-boron nitride conversion is thought to include a complex sequence of structural and chemical changes based on molecular rearrangements and evolution of dihydrogen which gradually created nanostructural boron nitride as depicted in Figure 1. In more detail, borazine is nebulized into a white aerosol, and the stream consisting of tiny borazine droplets suspended in the carrier gas is transported by the carrier gas to be passed through the preheated tubular furnace at 1400 °C. In the hot-zone, the formation of nanoparticles by SP of borazine can be understood as follows: the conversion of the nebulized precursor occurs through molecular condensation and ring-opening mechanisms involving evolution of dihydrogen and producing vapors of BN ring-based species. The latter, reacting to form the consolidated boron nitride network, are swept by the nitrogen carrier-gas flow and then condensed into a white product getting collected into the cooling traps near the outlet of the furnace. It should be mentioned that the conversion process generates significant amounts of H_2 which have to be continuously removed from the apparatus by an efficient nitrogen carrier-gas flow. As-trapped powders were immediately stored inside an argon-filled glovebox.

Scanning Electron Microscopy (SEM) of Ultrafine Powders. SEM is not really suited for observing nanosized materials, but it provides a view of the general particle population. The SEM image in Figure 1 (inset) shows that the particle population is relatively homogeneous including small particles which are of rounded shape and an extremely low proportion of particles with large size. It is therefore reasonable to suggest that the most important operating factors including the properties of the starting precursor, the pyrolysis temperature, the nitrogen flow rate, the residence time, and the heating rate of the droplet particles are controlled during processing.

Transmission Electron Microscopy (TEM) of Ultrafine Powders. The TEM micrograph of as-received powders was investigated to assess the morphology and the overall particle size of samples. An example of a characteristic TEM micrograph of as-synthesized powders is shown in Figure 2a. The low-magnification TEM bright field image shows that the sample forms elementary blocks which are composed of slightly agglomerated nanosized particles. The particle size ranges from 55 to 120 nm.

This agglomeration phenomenon is well-known for ultrafine powders and nanoparticles,[22,25,26] but we should point out that particles can be easily dispersed in acetone through ultrasonification with dispersion staying stable up to 96 h without sedimentation. As a consequence, it is reasonable to assume that the small particles are unaggregated.

The corresponding selected area electron diffraction (SAED) pattern, inset in Figure 2a, is composed of weak large diffraction rings which reveal a poorly crystallized BN phase. However, it should be mentioned that elementary blocks were deposited on a carbon coating for TEM observations; thereby the amorphous halo can result from this carbon coating. As a consequence, we investigated HRTEM to refine structural information and to corroborate SAED results. Figure 2b offers a high-resolution TEM (HRTEM) image which was used to gather information on powder nanostructure. The HRTEM image of the particle core demonstrates that the specimen consists of very fine nanocrystalline boron nitride (*nc*-BN) embedded in an amorphous boron nitride (*a*-BN). These *nc*-BN grains, in which sp^2 layers are significantly buckled in a disordered stacking sequence, exhibit size corresponding to less than 6 atomic basal planes, whereas their length does not exceed 50 Å.

X-ray Diffraction (XRD) of Ultrafine Powders. X-ray diffraction allowed assessment of the average crystallite size (ACS) and the interplanar distance d_{002} which both are indicative of the level of crystallinity of the BN phase. In XRD analysis, *h*-BN is identified by the presence of peaks at 26.76° (002), 41.60° (100), 43.87° (101), 50.15° (102), 55.16° (004), 75.93° (110), 82.18° (112), and 85.52° (105).[27] In a general way, two disordered BN phases, turbostratic-BN (*t*-BN) and amorphous-BN (*a*-BN), are found in addition to *h*-BN, and XRD patterns of such phases are significantly distinct

(25) Pratsinis, S. E. *Prog. Energy Combust. Sci.* **1998**, *24*, 197–219.
(26) Vemury, S.; Pratsinis, S. E. *J. Aerosol. Sci.* **1996**, *27*, 951–966.
(27) Pease, R. S. *Acta Crystallogr.* **1952**, *5*, 356–361.

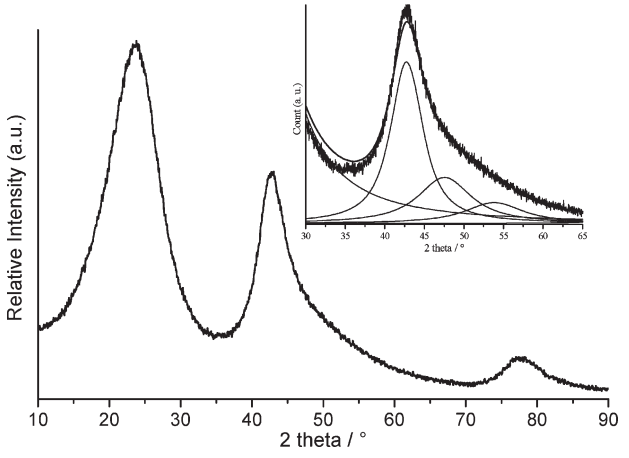

Figure 3. XRD pattern of as-synthesized ultrafine powders and Lorentz-type XRD pattern as the inset.

from that of *h*-BN.[28,29] Although difficulties have been encountered in analyzing the powders probably due to the very fine crystallite sizes which considerably broaden the XRD pattern (Figure 3), the layer disorder is evident from both the two-dimensional lattice type (10) reflection and the shift of the (002) reflection to lower angles (2θ = 24.10°) compared with *h*-BN. The XRD pattern reports only three peaks which can be attributed to the (002) plane, the (100)/(101)/(004) planes and the (110) plane. However, the resolution of the XRD pattern of powders is similar to those recorded for boron nitride powders with higher sizes obtained through a two-step process from oxygen-containing precursors.[12,13]

As a result of the poor resolution of the XRD pattern, difficulties arise to determine the ACS of powders. In particular, the accurate measurement of the in-plane coherence length ($\overline{L}_a$) is uncertain from the XRD pattern according to the fact that the peak corresponding to the (100) plane overlaps those which are attributed to (101) and (004) planes. To assess the average crystallite size in both *a* (in-plane coherence length, $\overline{L}_a$)- and *c* (out-plane coherence length, $\overline{L}_c$)-axes,[30] a deconvolution of the XRD pattern was performed, and the multipeak Lorentz function[31] was the best method to fit the experimental data. The Lorentz-type XRD pattern reported in Figure 3 as an inset is based on five Lorentz fitting peaks in the 2θ range 10−90°. We only reported the 2θ range 30−65° to display the separation of the (100), (101), and (004) peaks with deconvolution.

Consistently with a decrease in stacking order compared to *h*-BN, a d_{002} value of 3.68 Å has been calculated. Such a value confirms that the stacking sequence of the sp^2 layers is random and that the latter are disoriented around the *c*-axis. Samples also show low $\overline{L}_c$ and $\overline{L}_a$ values: $\overline{L}_c$ (obtained from the fwhm of the nondeconvoluated (002) peak[30a]) = 10 Å and $\overline{L}_a$ (obtained from the fwhm of the deconvoluated (100) peak[30a]) = 36.4 Å. As a consequence, the consolidation of the boron nitride structure is not fully achieved in as-synthesized powders. We therefore concluded that only partial crystallization takes place within the SP process of borazine at 1400 °C under nitrogen. To discuss these claims, FTIR, Raman, and chemical analyses have been investigated.

Infrared and Raman Spectroscopies and Composition of Powders. Figure 4a shows IR spectra of borazine and derived powders. A comparison of the spectra reveals that the bands corresponding to B−H (2509 cm^{-1}) and N−H (3451 and 897 cm^{-1}) bonds disappeared, whereas the absorption band of the B−N shifted and broadened on SP. The strong and broad absorption band centered at 1338 cm^{-1} and the sharp weak band at 787 cm^{-1} in powders are representative of the specific types of chemical bonds B−N in *h*-BN.[30,32]

These bands, which are assigned to the in plane ring vibration at 1368 cm^{-1} (E_{1u} mode) and out of the plane ring vibration at 805 cm^{-1} (A_{2u} mode) in *h*-BN, are significantly shifted in borazine-derived powders in relation with the partial occurrence of the crystallization process during SP. However, the absence of the bands corresponding to N−H and B−H bonds support the fact that borazine is fully converted into boron nitride in a chemistry point of view. This is reflected in the chemical composition of as-made powders. Results obtained by parallel bulk analytical techniques and EDX experiments give evidence that the bulk composition of powders is close to stoichiometric boron nitride despite the fact that each experiment gives slight quantitative differences. According to the bulk elemental analysis (H, <0.3 wt %; B, 44.4 wt %; N, 54.7 wt %; O, 0.8 wt %), we measured an empirical formula of $B_{1.0}N_{0.9}$ by omitting hydrogen and oxygen contents. EDX analysis revealed characteristic peaks for boron (0.18 keV), nitrogen (0.39 keV), and oxygen (0.523 keV) giving an empirical formula of $B_{1.0}N_{1.2}O_{0.1}$ (see Supporting Information SI.2). The detection of oxygen by EDX probably results from physisorbed/chemisorbed water. Despite differences in the B/N ratio, analysis provides evidence that the powders are pure, and we took into account the results from bulk analysis given an empirical formula of $B_{1.0}N_{0.9}$.

It can be concluded that the complex mechanistic sequence involving the design of the intermediate steps (to convert the sprayed borazine into *a*-BN powders) and the annealing treatments (to change *a*-BN powders into the desired final nanostructure, i.e., *h*-BN powders) has been stopped during the latter. The Raman spectrum of the product (Figure 4b) is in good agreement with such a postulate. The spectrum shows one peak at 1369.4 cm^{-1} (FWHM = 57.9 cm^{-1}) which is attributed to the E_{2g} vibration mode of *h*-BN (B−N in plane atomic

(28) Thomas, J. Jr.; Weston, N. E.; O'Connor, T. E. *J. Am. Chem. Soc.* **1963**, *84*, 4619–4622.
(29) Bernard, S.; Chassagneux, F.; Berthet, M. P.; Cornu, D.; Miele, P. *J. Am. Ceram. Soc.* **2005**, *88*, 1607–1614.
(30) (a) Bernard, S.; Chassagneux, F.; Berthet, M.-P.; Vincent, H.; Bouix, J. *J. Eur. Ceram. Soc.* **2002**, *22*, 2047–2059. (b) Bernard, S.; Ayadi, K.; Létoffé, J.-M.; Chassagneux, F.; Berthet, M.-P.; Cornu, D.; Miele, P. *J. Solid State Chem.* **2004**, *177*, 1803–1810.
(31) Breit, G.; Wigner, E. *Phys. Rev.* **1936**, *49*, 519–531.
(32) Nemanich, R. J.; Solin, S. A.; Martin, R. M. *Phys. Rev. B* **1981**, *23*, 6348–6356.

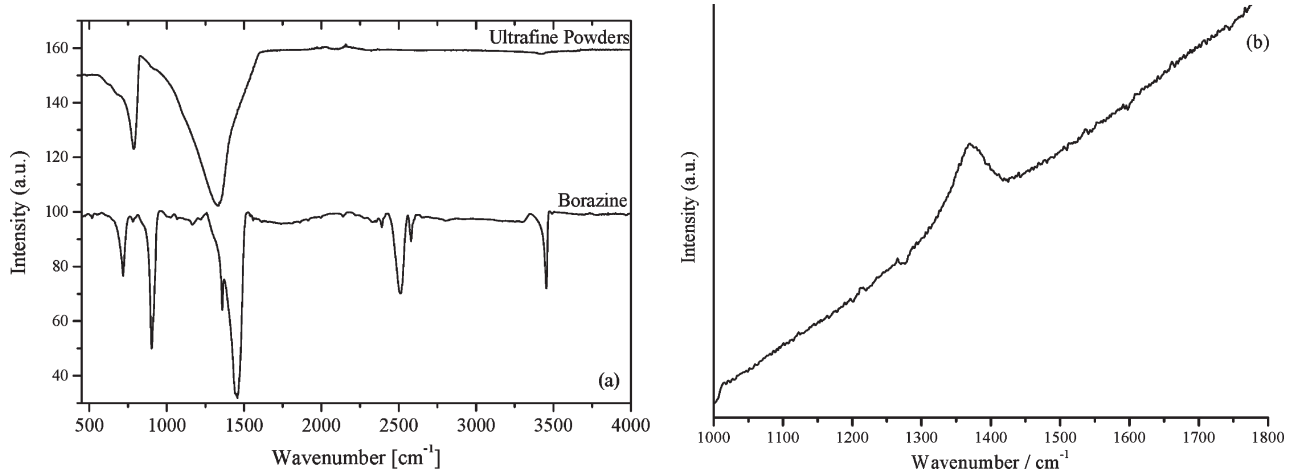

Figure 4. FTIR spectra of the borazine and derived powders (a) and Raman spectrum of powders (b).

displacements). This mode is located at 1368 cm^{-1} in polycrystalline *h*-BN powders.[32] Nemanish et al. showed that the peak corresponding to the E_{2g} vibration mode broadened and shifted to higher frequency as the crystallite size (L_a) decreased.[32] In our powders, this peak is shifted to a small increment, but the FHWM value is significantly higher than the one reported for micrometric powders (13 cm^{-1}) in ref 32. This corroborated definitely the fact that the crystallite size is very small in our powders. To confirm the nanometric size of powders measured by TEM, we investigated helium pycnometry and BET.

Helium Pycnometry, BET Specific Surface-Area (SSA), and Average Particle Sizes (APS) of Powders. According to the low degree of crystallization of powders, their density has been anticipated to be lower than the density of *h*-BN (d = 2.27 g cm^{-3}). The helium density of powders has been measured to be 1.95 ± 0.02 g cm^{-3}. This value can be compared to the density (1.85 g cm^{-3}) we found for BN fibers in a previous article.[30] It should be mentioned that density is closely related to both the pyrolysis process during which gaseous byproducts are removed (dihydrogen for sprayed borazine and probably low molecular weight species) and the crystallinity level of the corresponding BN materials. The density of precursor/polymer-derived boron nitride materials is commonly in the range 1.85−1.95 g cm^{-3},[2,30] whereas the density of boron (oxi-)nitride powders produced from organoborate precursors with diameters of 0.2−2 μm is in the range 1.55−2.1 g cm^{-3} after the first step of the two-step synthesis process.[12d] Taking into account such data, it is reasonable to consider that borazine-derived powders are relatively dense. In addition, the BET SSA value of 34.6 ± 0.7 m^2 g^{-1} is indicative of the low level of open porosity. Such a value is commonly found for nanosized powders.[22a,23−33] Equation 1 shows how the SSA and density (d) can be used to calculate the average particle size (APS in nm) of powders by assuming the spherical particle shapes:

$$\mathrm{APS} = 6000/(\mathrm{SSA} \times d) \quad (1)$$

An APS of 89 nm is calculated for borazine-derived powders confirming the local size measurement range made by TEM.

Ceramic Processing. The sintering of ultrafine $B_{1.0}N_{0.9}$ powders is a scientific and technological topic that affects the manufacture of bulk materials and the understanding of the stability of powders. Here, ultrafine $B_{1.0}N_{0.9}$ powders have been used to prepare dense boron nitride materials. However, the consolidation of such nanosized powders and more generally nitride materials without sintering additives has not been explored yet, probably because of the difficulties to prepare pure powders with small sizes and to sinter boron nitride without sintering additives. In the second part of this study, we therefore describe the preparation of highly dense boron nitride by additive-free sintering of the elementary building blocks containing the $B_{1.0}N_{0.9}$ particles as schematically depicted in Figure 5. This two-step process represents an alternative to the conventional solid-state route for the preparation of bulk boron nitride with inhomogeneous compaction and oxygen incorporation.

As previously mentioned, boron nitride is known to exhibit poor sinterability.[3,34] It is therefore required to use oxide sintering additives such as B_2O_3 and CaO to obtain boron nitride with a density approaching the density of pure boron nitride (~90%). However, it is not possible to obtain fully dense and impurity-free boron nitride in such conditions. In the present article, preliminary experiments showed that we succeeded in the preparation of highly dense and pure boron nitride by conventional sintering of ultrafine $B_{1.0}N_{0.9}$ powders without sintering additives. To our knowledge, it is the first time that 3D boron nitride materials are obtained by additive-free sintering. It should be mentioned that the preparation was made inside an argon-filled glovebox.

(33) (a) Hinklin, T.; Toury, B.; Gervais, C.; Babonneau, F.; Gislason, J. J.; Morton, R. W.; Laine, R. M. *Chem. Mater.* **2004**, *16*, 21–30. (b) Azurdia, J. A.; Marchal, J.; Shea, P.; Sun, H.; Pan, X. Q.; Laine, R. M. *Chem. Mater.* **2006**, *18*, 731–739.

(34) Masazumi, N.; Hiroshi, N.; Suminiko, K. U.S. Patent 5334339, August 2, **1994**.

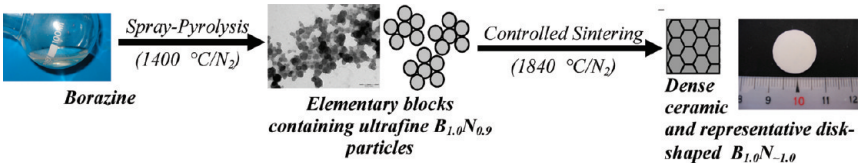

Figure 5. Schematic illustration of the approach for preparing highly dense boron nitride. The first step corresponds to the SP of borazine. The second step corresponds to the controlled sintering of the elementary blocks containing the $B_{1.0}N_{0.9}$ particles into a representative disk-shaped BN specimen.

$B_{1.0}N_{0.9}$ powders were first cold pressed with a load of 0.1 T and then heated under vacuum from RT to 600 °C before switching the vacuum to nitrogen atmosphere and increasing the temperature to 1100 °C. A pressure P_s (40 MPa) was applied during heating to 1840 °C. From 1100 °C, the temperature was monitored and regulated by an optical pyrometer focused on the surface of the die. After a dwelling time of 1 h at 1840 °C, the furnace was allowed to cool down at 8 °C min^{-1} with a gradual removal of the load to avoid appearance of cracks in the piece. The temperature dependence of the shrinkage for the sample indicated that ultrafine $B_{1.0}N_{0.9}$ powders started to densify at 1650 °C, with a densification kinetic reaching a maximum at 1750 °C. The densification rate was achieved at the beginning of the isothermal dwelling step (1840 °C). Therefore, sintering was stopped after 1 h. It is interesting to note that the applied sintering temperature is lower than those currently used for sintering boron nitride from micrometer or submicrometer sized counterparts.[3] This most probably results from the extremely small size and the high surface-to-volume ratio of $B_{1.0}N_{0.9}$ powders. Figure 5 shows a representative picture of a bulk boron nitride sample consolidated from nanosized $B_{1.0}N_{0.9}$ powders, then polished up to a 9 μm silicon carbide. The final dimension of the disk-shaped sample is 16 mm in diameter and approximately 2.4 mm in thickness, and the determined bulk composition after grinding inside a glovebox ($B_{1.0}N_{\sim 1.0}$; B = 44.3 wt %, N = 55 wt %, O = 0.7 wt %) is close to that determined for ultrafine $B_{1.0}N_{0.9}$ powders. This means that ultrafine $B_{1.0}N_{0.9}$ powders are relatively stable from a chemistry point of view. The specimen is free of macroscale defects such as circumferential or transversal cracks without apparent open porosity indicating sufficient compaction energy to obtain pore-free samples. Furthermore, optical micrographs of the polished specimen conventionally sintered at 1840 °C for 1 h (see Supporting Information SI.3) pointed to the fact that pull-out and/or cracking did not occur during polishing and that the boron nitride cylindrical part displayed an excellent machinability.

Attempts to consolidate $B_{1.0}N_{0.9}$ powders in ceramics by conventional sintering resulted in the formation of highly dense structures as illustrated by helium picnometry results. The helium density of powders has been measured to be 2.19 ± 0.001 g cm^{-3} giving a density of 96.3% of the theoretical density of *h*-BN (2.27 g cm^{-3}). It should be mentioned that measurements were performed on several parts of the sample presented in Figure 5 to examine piece homogeneity and to be representative of the specimen. Results were reproducible as reported in Supporting Information SI.4. In 1967, Kuznetsova and Poluboyarinov produced sintered boron nitride with an apparent density ranging from 2.06 and 2.08 g cm^{-3}, but the material was not pure due to the use of sintering additive.[35] Hubacek et al. studied the effect of the addition of copper in hot-pressed boron nitride.[3b,3c] Sintering of copper-free BN powders (0.64 μm) at 1950 °C with 30 MPa of pressure led to relative density of around 90%, but no details on the purity of starting boron nitride powders have been supplied. In the present paper, the use of ultrafine $B_{1.0}N_{0.9}$ powders allowed reaching the highest density in the derived bulk boron nitride specimens at a lower sintering temperature. Keeping in mind that the density is a key parameter for structural ceramics since it controls their strength and crack resistance to a high extent, such materials have a great potential.

Figure 6 reports representative micrographs of the fracture surface of sintered boron nitride prepared from ultrafine $B_{1.0}N_{0.9}$ powders. The SEM images of a fracture surface show a dense homogeneous and a nearly isotropic microstructure with BN grains facets (Figure 6a) having a slight parallel orientation with the sintering load axis. In Figure 6b, we can observe that the grain size is higher than the size of $B_{1.0}N_{0.9}$ particles indicating that grain growth occurred during sintering.

According to the fact that the SP of borazine at 1400 °C did not allow powders with high degree of crystallization (see HRTEM and XRD) to be obtained, it is clear that larger grains in the derived $B_{1.0}N_{\sim 1.0}$ samples are caused by recrystallization of metastable $B_{1.0}N_{0.9}$ powders during sintering. Therefore, we concluded that the sintering of ultrafine $B_{1.0}N_{0.9}$ powders at 1840 °C enhances the densification of bulk boron nitride but leads to uncontrollable grain growth causing the material to lose nanocrystalline characteristics. Grain growth is only limited by the surrounding grains. The microstructure of the bulk boron nitride is similar to that observed in the study of Hubacek and Ueki after a hot-pressing of commercially available BN submicropowders at 1950 °C with a load of 30 MPa.[3c]

The XRD pattern of the bulk $B_{1.0}N_{\sim 1.0}$ sample (Figure 7) considerably changed compared to the latter (Figure 3), whereas the infrared spectrum is identical (See Supporting Information SI.5) and the Raman spectrum does not exhibit peaks. For the latter, this is most probably due to luminescence effects which are more

(35) Kuznetsova, I. G.; Poluboyarinov, D. N. Refractories and Industrial Ceramics; Springer: New York, 1967; Vol. 8, pp 190−195.

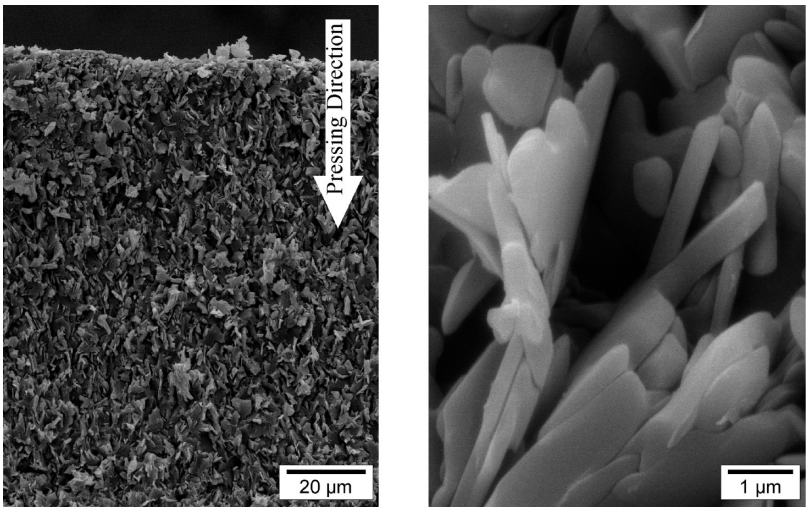

Figure 6. SEM micrographs of a representative bulk BN specimen.

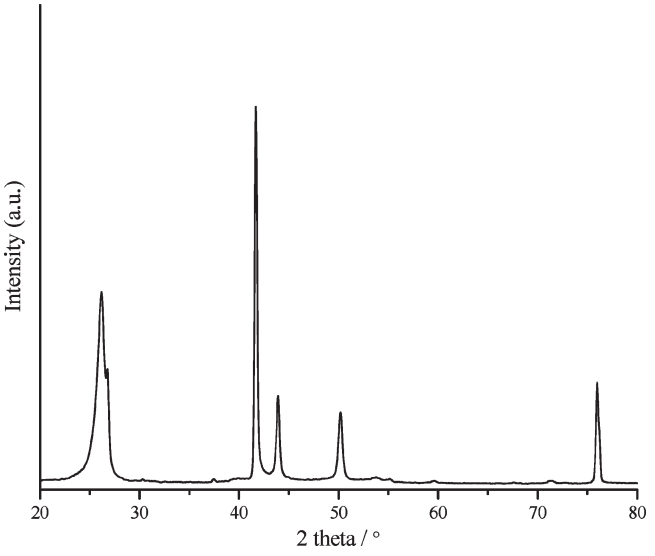

Figure 7. XRD pattern of a representative bulk specimen derived from ultrafine $B_{1.0}N_{0.9}$ powders.

pronounced in bulk materials. It should be mentioned that the disk-shaped boron nitride is placed in a position so that the pressing direction is perpendicular to the incidence plane for XRD experiments.

The XRD pattern of the bulk $B_{1.0}N_{\sim 1.0}$ sample exhibits the (*hkl*) peaks of *h*-BN in the 20−80° range with strong modification compared with the XRD pattern of ultrafine $B_{1.0}N_{0.9}$ powders (Figure 3). In particular, the initially unresolved (100)/(101)/(004) peak in ultrafine $B_{1.0}N_{0.9}$ powders (Figure 3) is clearly separated in the sintered boron nitride derived therefrom, while an additional (102) peak appeared. The appearance of additional peaks characteristic of *h*-BN is indicative of a strong enhancement in the structural ordering from ultrafine $B_{1.0}N_{0.9}$ powders to the bulk $B_{1.0}N_{\sim 1.0}$ sample. In support of these claims, we have compared the d_{002} spacing and the average crystallite sizes. The d_{002} spacing (d_{002} = 3.34 Å) is strongly reduced and relatively close to the theoretical value (3.327 Å). It corresponds to the spacing of

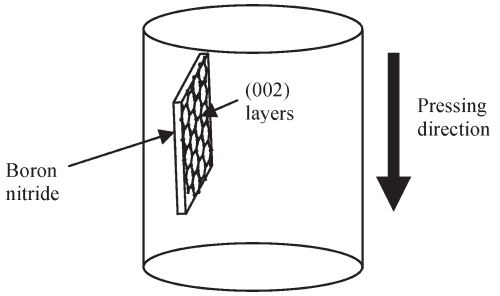

Figure 8. Orderly arrangement of the BN platenets in a representative bulk specimen.

relatively close-packed planes in a perfect *h*-BN crystal. The experimental (002) and (100) peaks are sharp ,which is the consequence of large crystallite sizes in the *c*- and *a*-axes ($\overline{L}_c$ = 88.8 Å, $\overline{L}_a$ = 615.9 Å). Besides, it is interesting to note that the (002) and (100) peaks respectively exhibited lower and higher intensities in comparison to the corresponding peaks in *h*-BN (JCPDS card No. 34-0421). This is supported by the low intensity of the (004) peak. Such observations indicated that (100) planes tend to be parallel to the X-ray beam, that is, perpendicular to the pressing direction, whereas (002) planes tend to be perpendicularly oriented to the surface, that is, parallel to the pressing direction. This confirmed SEM observations of the surface fracture (Figure 6) which highlighted a slight parallel orientation with the sintering load axis. As a consequence, the unidirectional hot pressing process probably results in the orderly arrangement of the boron nitride platelets parallel to the pressing direction as illustrated in Figure 8. This can affect the mechanical properties of sintered boron nitride. In this regard, the microhardness of samples was measured.

An average value of 8 HV (78 MPa) was found for the microhardness throughout the cross-section. However, there is a lack of evidence or discussion in the literature to support our contentment with regards to microhardness of sintered boron nitride. Hubacek and Ueki[3c] obtained a range of mean values starting from 15 to approximately

28 Hv for copper-activated hot-pressed boron nitride. More recently, a calculation gave a rough estimate of the BN theoretical hardness value.[36] In the latter, authors demonstrated that the theoretical hardness value of 130−160 MPa for *h*-BN crystal is controlled by the cleavage of the van der Waals bonds between the (002) layers. Taking into account that the hardness measurements have been performed in a direction parallel to the pressing direction and that (002) layers tend be oriented parallel to the pressing direction in bulk $B_{1.0}N_{\sim 1.0}$ samples, the HV value is probably minimized in our case in this direction.

Conclusion

The SP process of borazine followed by an additive-free sintering of derived ultrafine $B_{1.0}N_{0.9}$ powders have been combined for the first time to process pure bulk boron nitride ($B_{1.0}N_{\sim 1.0}$) with a very high density and a homogeneous microstructure. This two-step process represents a novel approach to generate dense, crack-free, and pure bulk hexagonal−boron nitride materials at temperatures lower than those reported for micrometer or submicrometer counterparts. Grain growth occurred during sintering leading to a micrograined sintered $B_{1.0}N_{\sim 1.0}$ product and probably causing the macroscopic material to lose the nanocrystalline characteristics of $B_{1.0}N_{0.9}$ powders.

A major challenge in the preparation of bulk materials from nanosized particles is the limitation of grain growth during sintering. In our case, we suggest to overcome this problem, that is, control the metastable-to-stable transition phase, to some extent through three methods which are under investigation. Very high densification and controlled grain growth could be obtained by a careful optimization of the sintering process using the spark plasma sintering process. SPS enables a powder compact to be sintered to high density at relatively low temperatures and in short time, typically a few minutes, in comparison to conventional sintering. The second method focuses on the enhancement of the crystallinity level of $B_{1.0}N_{0.9}$ powders to avoid recrystallization during further sintering, and the third method is to investigate the pressure applied during sintering which is another variable that strongly influences the final grain size of a sintered product.

An important aspect of the current research is the extension of the underlying processing method to a wider range of nonoxide materials including binary systems, nanocomposites, and solid solutions. To date, the combination of SP of oxygen-free molecules and sintering of derived ultrafine nonoxide nanopowders has never been applied to prepared 3D nonoxide materials. However, because of the versatility of SP, this two-step approach should open the way to a very broad set of nonoxide materials using single-source molecules or a dual source. These opportunities are now being addressed. It is anticipated that this will lead to a host of structural and functional applications for a new generation of materials.

Acknowledgment. We gratefully acknowledge the CTμ (Centre Technologique des Microstructures) of the Université Lyon 1 for access to the SEM apparatus and Mikhael Bechelany from Swiss Federal Laboratories for Materials Testing and Research (EMPA), Laboratory of Nanostructures and Mechanics (Thun, Switzerland) for EDX experiments.

Supporting Information Available: ^{1}H NMR and FTIR spectra of the borazine, EDX data of as-synthesized ultrafine powders, optical micrographs of the polished surfaces of boron nitride ceramics, reproducibility of the density for bulk $B_{1.0}N_{\sim 1.0}$ samples, and ATR-FTIR spectrum for the sintered boron nitride (PDF). This material is available free of charge via the Internet at http://pubs.acs.org.

(36) Petrescu, M. I. *Diamond Relat. Mater.* **2004**, *13*, 1848–1853.